This article was downloaded by: [Institute Of Atmospheric Physics]
On: 09 December 2014, At: 15:17
Publisher: Taylor & Francis
Informa Ltd Registered in England and Wales Registered Number: 1072954 Registered office: Mortimer House, 37-41 Mortimer Street, London W1T 3JH, UK

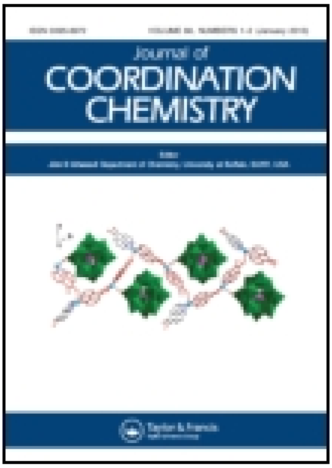

Click for updates

Journal of Coordination Chemistry
Publication details, including instructions for authors and subscription information:
http://www.tandfonline.com/loi/gcoo20

Study on the reactions of zinc carboxylate complexes with copper(II) or cobalt(II) ions

Bo Xiao[a], Hai-Yang Xiao[b] & Min-Dong Chen[a]
[a] Jiangsu Key Laboratory of Atmospheric Environment Monitoring and Pollution Control, School of Environmental Science and Engineering, Nanjing University of Information Science and Technology, Nanjing, PR China
[b] Henan Provincial Key Laboratory of Surface and Interface Science, Zhengzhou University of Light Industry, Zhengzhou, PR China

Accepted author version posted online: 24 Jun 2014.Published online: 18 Jul 2014.

To cite this article: Bo Xiao, Hai-Yang Xiao & Min-Dong Chen (2014) Study on the reactions of zinc carboxylate complexes with copper(II) or cobalt(II) ions, Journal of Coordination Chemistry, 67:14, 2455-2469, DOI: 10.1080/00958972.2014.937710

To link to this article: http://dx.doi.org/10.1080/00958972.2014.937710

PLEASE SCROLL DOWN FOR ARTICLE

Taylor & Francis makes every effort to ensure the accuracy of all the information (the "Content") contained in the publications on our platform. However, Taylor & Francis, our agents, and our licensors make no representations or warranties whatsoever as to the accuracy, completeness, or suitability for any purpose of the Content. Any opinions and views expressed in this publication are the opinions and views of the authors, and are not the views of or endorsed by Taylor & Francis. The accuracy of the Content should not be relied upon and should be independently verified with primary sources of information. Taylor and Francis shall not be liable for any losses, actions, claims, proceedings, demands, costs, expenses, damages, and other liabilities whatsoever or howsoever caused arising directly or indirectly in connection with, in relation to or arising out of the use of the Content.

This article may be used for research, teaching, and private study purposes. Any substantial or systematic reproduction, redistribution, reselling, loan, sub-licensing, systematic supply, or distribution in any form to anyone is expressly forbidden. Terms &

Journal of Coordination Chemistry, 2014
Vol. 67, No. 14, 2455–2469, http://dx.doi.org/10.1080/00958972.2014.937710

Study on the reactions of zinc carboxylate complexes with copper(II) or cobalt(II) ions

BO XIAO*†, HAI-YANG XIAO‡ and MIN-DONG CHEN*†

†Jiangsu Key Laboratory of Atmospheric Environment Monitoring and Pollution Control, School of Environmental Science and Engineering, Nanjing University of Information Science and Technology, Nanjing, PR China
‡Henan Provincial Key Laboratory of Surface and Interface Science, Zhengzhou University of Light Industry, Zhengzhou, PR China

(*Received 20 December 2013; accepted 16 May 2014*)

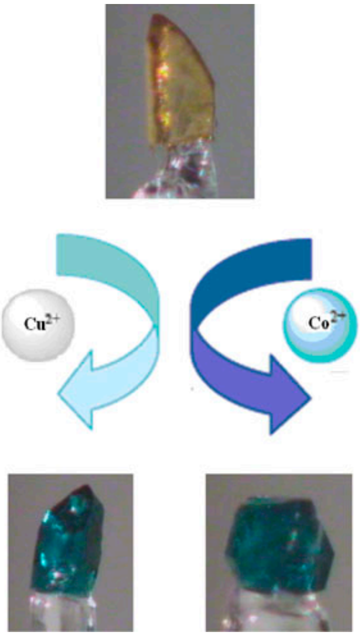

By immersion of selected big single crystals of $[Zn(pc)(Phen)(H_2O)]_2{\cdot}6H_2O$ (**1**; $H_2pc = $ 4-hydroxyphthalic acid) into aqueous solutions of $Cu(NO_3)_2$ and $Co(NO_3)_2$, respectively, two central metal ion exchange induced SCTSC transformation products, $[Cu_{0.63}Zn_{0.37}(pc)(Phen)(H_2O)]_2{\cdot}6H_2O$ (**2**) and $[Co_{0.69}Zn_{0.31}(pc)(Phen)(H_2O)]_2{\cdot}6H_2O$ (**3**), can be obtained. As heterogeneous catalysts, central metal ion-exchanged products **2** and **3** showed high catalytic efficiency in the green oxidative polymerization of DMP. Our results indicate that central metal ion exchange might be regarded as a powerful and effective method to modify properties of crystalline materials only by varying central metal ions under moderate conditions.

---

*Corresponding authors. Email: boxiao_nuist@163.com (B. Xiao); chenmd@nuist.edu.cn (M.-D. Chen)

Reaction of zinc carboxylate, $[Zn(pc)(Phen)(H_2O)]_2 \cdot 6H_2O$ (**1**; H_2pc = 4-hydroxyphthalic acid), with $Cu(NO_3)_2$ or $Co(NO_3)_2$ is investigated. By immersion of single crystals of **1** into aqueous solutions of $Cu(NO_3)_2$ and $Co(NO_3)_2$, respectively, metal ion exchange induced single-crystal to single-crystal (SCTSC) transformation products, $[Cu_{0.63}Zn_{0.37}(pc)(Phen)(H_2O)]_2 \cdot 6H_2O$ (**2**) and $[Co_{0.69}Zn_{0.31}(pc)(Phen)(H_2O)]_2 \cdot 6H_2O$ (**3**), could be obtained. As heterogeneous catalysts, central metal ion-exchanged products **2** and **3** show high catalytic efficiency in the green oxidative polymerization of 2,6-dimethylphenol (DMP) to poly(1,4-phenylene ether) in the presence of H_2O_2 as oxidant in water under mild conditions with reuse without significant loss of activity through three runs, which suggests that these catalysts are efficient, mild, and easily recyclable for the oxidative coupling of DMP. Our results indicate that central metal ion exchange might be a powerful and effective method to modify properties of crystalline materials by varying the central metal ions under moderate conditions.

Keywords: Single-crystal to single-crystal (SCTSC) transformation; Oxidative coupling; Heterogeneous catalyst; Green chemistry

1. Introduction

Poly(1,4-phenylene ether) (PPE) as an engineering plastic has been widely used in various areas, such as business equipment and electrical and automotive industries. The oxidative polymerization of 2,6-dimethylphenol (DMP) to form PPE was first carried out by Hay and his GE group in 1959 with a copper–pyridine complex as a catalyst in nitrobenzene solution [1]. Along with the formation of PPE by C–O coupling, an undesirable byproduct, 3,3′,5,5′-tertramethyl-4,4′-diphenoquinone (DPQ), was also produced by C–C coupling of two monomeric phenols. Although the oxidative polymerization of DMP in organic solvents has provided a convenient method for manufacturing PPE in the industry, both a solvent-recovery process and an anti-explosive reactor are required in the industrial production of PPE [2]. From the view of green chemistry, the use of water as a reaction medium is environmentally friendly and PPE can easily be separated from water due to its insolubility in water [3, 4]. In 2004, Nishide *et al.* first used potassium ferricyanide as an oxidant to synthesize PPE in alkaline water. Unfortunately, the use of potassium ferricyanide is still environmentally deleterious [5]. Green oxidative coupling of DMP in environmental friendly solvents with clean oxidants is extremely rare. Therefore, this reaction is still a great challenge from the standpoint of “green chemistry and technology.”

Organic–inorganic hybrid materials have received attention owing to their potential applications in adsorption and separation processes, ion exchange, catalysis, and sensor technology [6–9]. One of the salient features of hybrid materials is that they often contain substitution-active metal sites in their framework, and the metal centers are incorporated in the interstitial or porous coordination network, making such materials better for ion exchange [10]. Other coordination-driven metal ions will be capable of entering the interstices or pores (cavities) and reacting with substitution-active metal sites, and then it might be applied to cation exchange materials [11], which can effectively remove some highly toxic heavy metals. The central metal ion exchange process is, however, seldom observed by single-crystal X-ray diffraction (XRD) studies because possible drastic structural changes during the process cause loss of crystallinity. Retaining single crystallinity even after the occurrence of exchange reactions is very important for the development and study of central metal ion exchange materials [12]. Recent studies show that [13], through exchange of central metal ion, the framework integrity of some porous metal phosphonate, carboxylate, and sulfonate complexes can be maintained. Hence, exchange of the central metal ion in porous complexes can be utilized to design some new metal ion exchange materials. This is a promising strategy for the synthesis and design of solid materials, which could be done by immersing some selectable stable big crystals into the aqueous solution of a certain metal salt and generating the replacement of cations. In order to further investigate the coordination-driven central metal ion exchange reaction, we synthesize a zinc carboxylate $[Zn(pc)(Phen)(H_2O)]_2·6H_2O$ (**1**, H_2pc = 4-hydroxyphthalic acid). Through single-crystal to single-crystal (SCTSC) transformation, $[Cu_{0.63}Zn_{0.37}(pc)(Phen)(H_2O)]_2·6H_2O$ (**2**) and $[Co_{0.69}Zn_{0.31}(pc)(Phen)(H_2O)]_2·6H_2O$ (**3**) are obtained. In addition, we explore their application as catalysts for an aqueous-medium catalysis process of the oxidative coupling of DMP using hydrogen peroxide as oxidant under mild conditions.

2. Experimental

2.1. *General information and materials*

All solvents and chemicals (analytical grade) were used without purification. 4-Hydroxyphthalic acid (H_2pc), Phen, and DMP (99% pure) were used as obtained from J&K Chemical Ltd. Elemental analyses (C, H, and N) were performed on a Perkin–Elemer 240C analyzer. IR spectra were recorded from 4000 to 400 cm^{-1} on a Tensor 27 OPUS (Bruker) FT-IR spectrometer with KBr pellets. The X-ray powder diffraction patterns were recorded on a Rigaku D/Max-2500 diffractometer, operated at 40 kV and 100 mA, using a Cu-target tube and a graphite monochromator. The intensity data were recorded by continuous scan in a $2\theta/\theta$ mode from 3° to 80° with a step size of 0.02° and a scan speed of $8°\,min^{-1}$. Atom adsorption analysis was conducted on a Hitch Z-8000 atom adsorption analyzer. Field emission scanning electron microscopy (SEM) and energy dispersive X-ray spectrometry (EDS) were conducted on a JSM-6490 scanning electron microscope. Atomic force microscopy (AFM) images were taken with a silicon nitride scanning tip (Nanoprobe, Veeco Metrology Group, Santa Barbara, CA).

2.2. *Synthesis of $[Zn(pc)(Phen)(H_2O)]_2·6H_2O$ (1)*

To a stirred solution of 2 equiv. of $Zn(NO_3)_2·6H_2O$ (29.7 mg, 0.1 mM) in H_2O (5 mL) was added 2 equiv. of phen (18.0 mg, 0.1 mM) in CH_3OH (5 mL). After stirring for 5 min, a solution of 4-hydroxyphthalic acid (18.2 mg, 0.1 mM) in CH_3OH (5 mL) was added, and the mixture was then stirred for 10 min. Upon evaporation of the solvent, straw yellow block crystals were isolated in 56% yield. Anal. Calcd for $C_{40}H_{26}N_4O_{18}Zn_2$: C, 48.95; H, 2.67; N, 5.71%. Found (%): C, 48.86; H, 2.79, N, 5.59; IR (KBr)/cm^{-1}: 3507(m), 3083(m), 2680(w), 1551(s), 1389(s), 1306(m), 1266(m), 1161(w), 1066(w), 874(m), 729(m), 635(w), 452(w).

2.3. *Synthesis of $[Cu_{0.63}Zn_{0.37}(pc)(Phen)(H_2O)]_2·6H_2O$ (2)*

Several big single crystals of **1** (0.010 g) were immersed in 5 mL of a 1 $mg\,mL^{-1}$ aqueous solution of $Cu(NO_3)_2·3H_2O$. After 5 days, green exchanged crystals were obtained at room temperature. The crystals are stable in air. Anal. Calcd for $C_{40}H_{40}Cu_{1.26}N_4O_{18}Zn_{0.74}$: C, 48.33; H, 4.03; N, 5.64%. Found (%): C, 48.52; H, 3.84; N, 5.53; IR (KBr)/cm^{-1}: 3464(m), 1683(s), 1609(m), 1374(m), 1326(m), 1221(w), 986(w), 882(w), 806(w), 776(m), 676(m), 446(w).

2.4. *Synthesis of [$Co_{0.69}Zn_{0.31}$(pc)(Phen)(H_2O)]$_2$·6H_2O (3)*

According to the synthetic method of **2**, complex **3** was prepared through use of aqueous solution of $Co(NO_3)_2·6H_2O$ instead of aqueous solution of $Cu(NO_3)_2$. After 5 days, green exchanged crystals were obtained at room temperature. The crystals are stable in air. Anal. Calcd for $C_{20}H_{20}Co_{0.69}N_2O_9Zn_{0.31}$: C, 48.69; H, 4.09; N, 5.68%. Found (%): C, 48.82; H, 3.94; N, 5.61; IR (KBr)/cm^{-1}: 3434(w), 1645(s), 1543(m), 1448(s), 1348(m), 1285(w), 1145(w), 1076(w), 879(w), 739(w), 552(m), 439(w).

2.5. *X-ray structure analyses*

X-ray single-crystal diffraction measurements for **1–3** were carried out on a Bruker Smart 1000 CCD diffractometer equipped with a graphite crystal monochromator situated in the incident beam for data collection at 293(2) K. The determinations of unit cell parameters and data collections were performed with Mo Kα radiation ($\lambda = 0.71073$ Å), and unit cell dimensions were obtained with least-square refinements. The program SAINT [14] was used for integration of the diffraction profiles. Semi-empirical absorption corrections were applied using SADABS [15]. All structures were solved by direct methods using the SHELXS program of the SHELXTL package and refined with SHELXL [16]. Metal atoms in each complex were located from the E-maps, and other non-hydrogen atoms were located in successive difference Fourier syntheses and refined with anisotropic thermal parameters on $|F|^2$. Hydrogens were added theoretically, riding on the concerned atoms and refined with fixed thermal factors. Table 1 shows crystal data and processing parameters for all complexes.

2.6. *Experimental procedure for the catalytic oxidative coupling of DMP [17]*

One micro mole of DMP (122 mg) was dissolved in 5 mL of water containing 1 mM of NaOH (40 mg) and 0.1 mM of sodium dodecyl sulfate (SDS) (29 mg). 0.02 mM of complex

Table 1. Crystal data and structure refinement for [Zn(pc)(Phen)(H_2O)]$_2$·6H_2O (**1**), [$Cu_{0.63}Zn_{0.37}$(pc)(Phen)(H_2O)]$_2$·6H_2O (**2**), and [$Co_{0.69}Zn_{0.31}$(pc)(Phen)(H_2O)]$_2$·6H_2O (**3**).

	1	**2**	**3**
Formula	$C_{40}H_{26}N_4O_{18}Zn_2$	$C_{40}H_{40}Cu_{1.26}N_4O_{18}Zn_{0.74}$	$C_{20}H_{20}Co_{0.69}N_2O_9Zn_{0.31}$
Formula weight	981.39	993.19	493.28
Crystal system	Monoclinic	Monoclinic	Monoclinic
Space group	*C2/c*	*Cs*	*C2/c*
a (Å)	20.3369(9)	20.3425(6)	20.3388(11)
b (Å)	11.9924(5)	11.9948(4)	12.0040(6)
c (Å)	16.1999(7)	16.1943(5)	16.2042(9)
α (°)	90.00	90	90.00
β (°)	94.278(4)	94.303(2)	94.295(5)
γ (°)	90.00	90	90.00
V (Å^3)	3940.0(3)	3940.3(2)	3945.1(4)
T (K)	293(2)	291(2)	293(2)
Z	4	4	8
μ(Mo Kα) (cm^{-1})	1.306	1.219	1.044
No. of reflections collected [$I > 2\delta(I)$]	4014	4013	3676
No. of independent reflections	2862	3144	2617
Final R^a, R^w	0.0596, 0.1728	0.0458, 0.1185	0.0672, 0.1897

with appropriate size was added to the above solution and the mixture was stirred at 50 °C. Then, 10 μL of H_2O_2 (30% aqueous solution) was slowly added into the mixture using a micro-injector every 15 min (two times in all). After 8 h, the reaction was stopped and 1.17 g of NaCl was added. Then, the mixture was transferred into a separatory funnel and the organic materials were extracted with $CHCl_3$ three times. The combined organic extracts were dried with anhydrous $MgSO_4$ and the filtrate was evaporated in vacuum. The products were separated by preparative TLC performed on dry silica gel plates with ethyl ether/petroleum ether (1 : 3 v/v) as the developing solvent. The main product, PPE, and byproduct, DPQ, were collected and dried in vacuum, respectively.

The crystal complex catalysts were powdered to increase the surface area for the catalysts prior to use. Under air, the substrate DMP (0.122 g, 1 mM) was dissolved in 1 : 1 (v/v, 5 mL) mixture of methanol–toluene in a 10 mL flask, and a 2% molar ratio of catalyst/substrate and a 7 M ratio of NaOMe/catalyst were added with a magnetic stirrer. Then, hydrogen peroxide (30% aqueous solution) was slowly added into the mixture using a syringe pump every 15 min (10 μL for five times) to minimize H_2O_2 decomposition. After 3 h, the sample was concentrated in vacuum and the products were separated by preparative TLC performed on dry silica gel plates. All reactions were run in duplicate and the data reported represent the average of these reactions.

Poly(phenylene ether) (PPE): ^1H NMR ($CDCl_3$, TMS) $\delta = 6.44$ (s, 2H; H_{Ar}), 2.09 ppm (s, 6H; CH_3); ^{13}C NMR ($CDCl_3$, TMS) $\delta = 16.6$–16.8, 114.1, 114.5, 124.4, 125.0, 129.0, 131.6, 132.7, 145.6, 146.4, 151.5, 154.5, 154.8 ppm; IR (KBr): $\bar{\nu}_{C\text{–}O\text{–}C} = 1186\ cm^{-1}$.

DPQ: ^1H NMR ($CDCl_3$, TMS) $\delta = 8.2$ (s, 4H), 7.1 (s, 2H), 2.1 ppm (12H); ^{13}C NMR ($CDCl_3$, TMS) $\delta = 17.07$, 129.56, 135.67, 139.10, 187.21 ppm; IR (KBr): $\bar{\nu}_{C=O} = 1594\ cm^{-1}$.

2.7. *Ion exchange test*

The effect of the initial concentration of Cu(II) on copper ion exchange was also examined. Ten milligrams of crystalline **1** was immersed in 5 mL of an aqueous solution of $Cu(NO_3)_2$, the concentration of which ranged from 0.2 to 1 mg mL^{-1}, in a glass tube. The tubes were allowed to stand for five days at room temperature. Then the resultant crystalline materials were filtered, washed with deionized water, and dissolved in HNO_3 solution. The final concentrations of Cu(II) in the resultant crystalline materials were measured using a Hitch Z-8000 atom adsorption analyzer.

3. Results and discussion

3.1. *Crystal structure of [Zn(pc)(Phen)(H_2O)]$_2$·6H_2O (1)*

Crystallographic analysis reveals that **1** crystallizes in the monoclinic space group *C2/c* as the dinuclear neutral molecule [Zn(pc)(Phen)(H_2O)]$_2$. The asymmetric unit consists of two Zn^{2+} ions, two phen ligands, two deprotonated pc^{2-} ions, two coordinated waters, and six lattice water molecules. Each Zn(II) is a five-coordinate with two nitrogens of one phen and three oxygens from two different deprotonated pc^{2-} ligands and one coordinated water, forming a distorted trigonal bipyramidal geometry, where N1, N2, and O1 locate at the equatorial positions, while O6 and O2A occupy the axial positions (figure 1). The

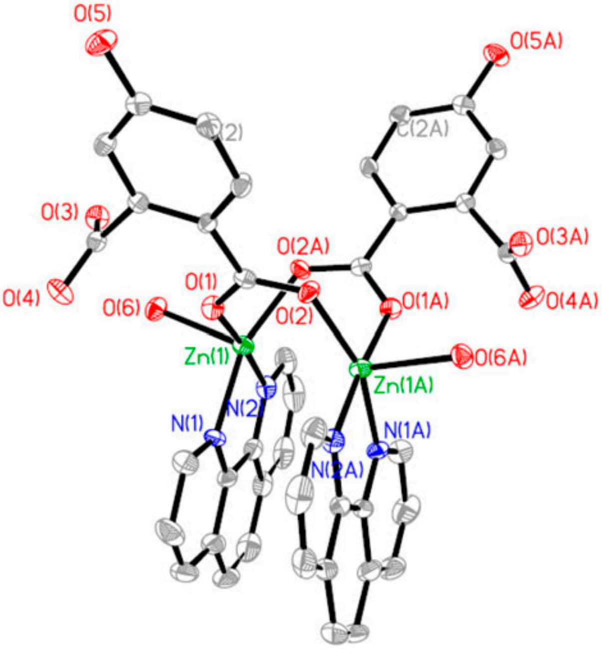

Figure 1. Molecular structure of **1** with atom labeling of the asymmetric unit. All hydrogens are omitted for clarity.

d(Zn–$O_{carboxylate}$) is 1.936(3)–1.993(3) Å and d(Zn–O_{water}) is 2.174(3) Å, in the range of typical Zn–O (carboxylate and water) distances [18]. The Zn–N bond lengths are 1.986(4) and 2.013(4) Å. The distorted trigonal bipyramid ZnO_3N_2 has O(N)–Zn–O(N) angles ranging from 90.07(14)° to 174.54(15)°, within the range expected for such coordination. Each pc^{2-} connects adjacent Zn(II) centers to form a dimer in a bidentate bridging mode by one of the two carboxylate groups with Zn···Zn separation of 3.1088(10) Å and another carboxylate group is free of coordination, while Phen is typical chelating the Zn(II). Hydrogen bonding interactions are usually important in the synthesis of supramolecular architecture. There exist O–H···O hydrogen bonding interactions between lattice waters, coordinated water, and carboxyl oxygens with distances of 2.630(4)–3.40(2) Å, leading to the formation of a 2-D supramolecular network.

3.2. *Central metal ion exchange induced SCTSC transformation*

Central metal ion exchange properties of organic–inorganic hybrid materials are closely associated with the coordination ability of the metal ions [13(b)]. Due to the strong coordination ability of copper or cobalt ions to carboxylate [19], copper or cobalt could partly replace the central zinc ions in **1**. **1** cannot dissolve in H_2O, CH_3COCH_3, and CH_3CN, but can slightly dissolve in C_2H_5OH and can dissolve in THF, hot CH_3OH, DMF, and DMSO. We first investigate the influence of concentrations of $Cu(NO_3)_2$ (from 0.2 to 1 mg mL^{-1}) on the percentage of exchanged zinc ions. As shown in figure 2, the percentage of exchanged zinc ions in concentrated solutions of $Cu(NO_3)_2{\cdot}3H_2O$ is slightly greater than those in dilute solutions. For example, the percentage is 63.12% in 1 mg mL^{-1} solution of

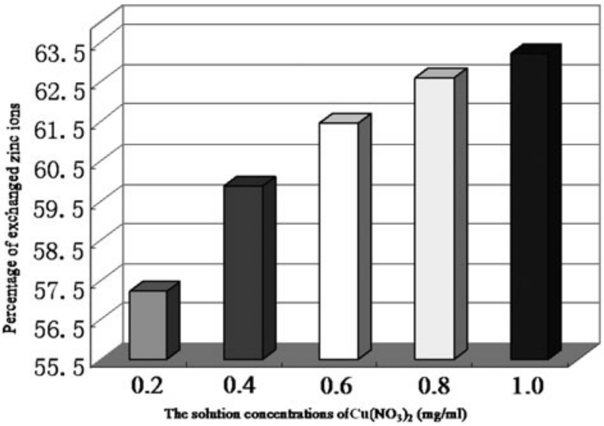

Figure 2. The percentage of exchanged zinc ions of crystalline **1** in different solution concentration of copper nitrate.

$Cu(NO_3)_2$, whereas the percentages are 59.79% in 0.4 mg mL^{-1} solution of $Cu(NO_3)_2$ and 57.13% in 0.2 mg mL^{-1} solution of $Cu(NO_3)_2$. The rising trend of the percentage gradually becomes slow, which indicates that the percentage of exchanged zinc ions would be finite. Subsequently, Cu-exchanged induced product $[Cu_{0.63}Zn_{0.37}(pc)(Phen)(H_2O)]_2\cdot 6H_2O$, **2**, is obtained by immersing big crystals of **1** into an aqueous solution of 1 mg mL^{-1} copper nitrate for five days. From a photograph of the crystal (figure 3), we can clearly see that **2** entirely maintains single crystallinity. XRD confirms that a SCTSC transformation has occurred, resulting in a Cu–Zn complex, and the complex retains the same structure as **1**. As shown in figure 4, analogous powder X-ray diffraction (PXRD) analysis and IR spectra also verify that the exchanged product **2** retains **1**'s structure. Complex **2** is carefully analyzed using an atomic adsorption spectrophotometer, and the content of zinc is 36.76%, while that of copper is 63.24%. These results agree well with elemental analysis. Similar to **2**, Co-exchanged product $[Co_{0.69}Zn_{0.31}(pc)(Phen)(H_2O)]_2\cdot 6H_2O$, **3**, can also be prepared by immersing the big crystals of **1** into an aqueous solution of 1 mg mL^{-1} cobalt nitrate for five days. Complex **3** also inherits the single crystallinity and crystal structure of **1**. Analogous XRD analysis and IR spectra (figure 4) also verify that **3** retains **1**'s structure. The contents of zinc and cobalt are 31.09 and 68.91%, respectively, which are measured by atomic adsorption and confirmed by elemental analysis. Obviously, it is the coordination ability of the in-going metal ions toward ligands that controls the reaction process of central metal ion exchange. If the coordination ability of the in-going metal ions is close to or roughly similar to that of the central metal ions, the cation-exchanged products will preserve the original structure to a great extent, as in the case of **2** and **3**.

To further clarify the central metal ion exchange, energy dispersive X-ray spectroscopy (EDS) measurements on **2** and **3** are carried out. Figure 5(a) shows the SEM and EDS results of the crystal surface of **2**. The detected surface atom ratios for carbon, nitrogen, oxygen, copper, and zinc are 51.46, 9.65, 20.40, 16.67, and 1.84%, respectively. After this crystal is cut [figure 5(b)], the interior atom ratios of the crystal for carbon, nitrogen, oxygen, copper, and zinc are 40.23, 7.19, 39.33, 9.25, and 4.00%, respectively. Obviously, the percentage of exchanged zinc ions on the surface of **2** is slightly greater than that in the interior, and the mean value of EDS results accord with atomic adsorption spectrophotometer

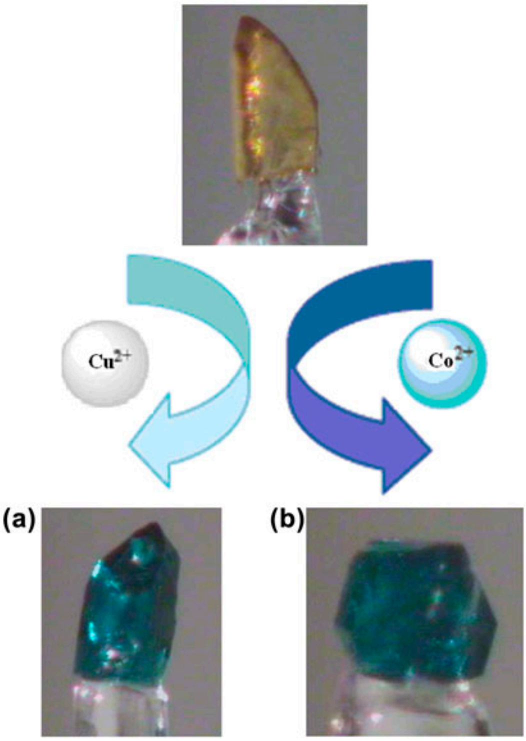

Figure 3. Photographs of **1**'s single crystal in central metal ion exchange process. (a) {Zn, 37%; Cu, 63%} and (b) {Zn, 31%; Co, 69%}.

and elemental analysis. Analogous results also occur in **3** (figure 6). These results are similar to a previous report [13(c)], where there is a diminishing concentration gradient of Fe(III) from the crystal surface to the interior. It indicates that there is some resistance to both external mass transfer and intra-particle diffusion.

Micro-topographic AFM is a technique that is used for further identifying SCTSC transformation in a dynamic regime [20]. Usually, a dissolution–reprecipitation process [21] will occur in the course of ion exchange, and the formation of a new crystalline phase on the surface of the old one starts, which continues until the ion exchange is complete. Meanwhile, the height of microcrystallites (or peaks or holes [22]) becomes more pronounced and complexes will rapidly lose their crystallinity turning opaque [23]. This loss of singularity, which indicates a significant restructuring of the crystal in conjunction with changes in the crystallographic symmetry of the complex, is, to us, inconsistent with the proposed SCTSC process. If the crystal surface profile or height of microcrystallites has no obvious change, we think that it will be a SCTSC process. The AFM technique is a good method that can be utilized to image the crystal surface profile to reveal nanoscopic features on the surface. From figure 7, we can see that the crystal surface profiles and peak heights of AFM images of **1** and **2** show no obvious change, which indicates a SCTSC process. During the course of ion exchange, we cannot find a dissolution–reprecipitation process. Similar phenomena also occur between **1** and **3**.

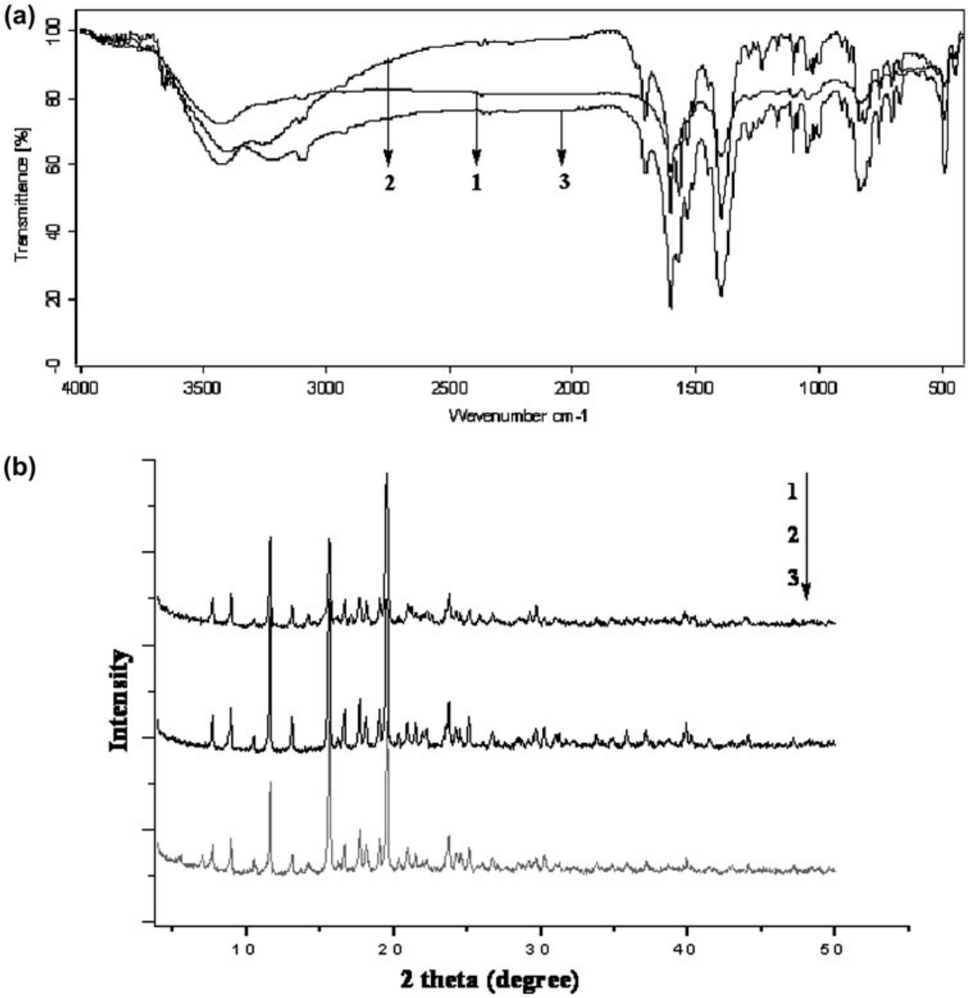

Figure 4. (a) IR spectra of **1** and its Cu(II), Co(II)-exchanged products (**2** and **3**). (b) PXRD patterns of **1** and its Cu(II), Co(II)-exchanged products (**2** and **3**).

3.3. *Catalytic oxidative coupling of DMP in water*

The overall oxidative coupling process of DMP under green reaction conditions is shown in scheme 1. Under the same reaction conditions, the catalytic activities of the Zn(II) dimer **1** and its cation-exchanged products **2** and **3** possess big differences, though they have the same structures. As can be seen in table 2, Cu-exchanged product **2** has better activity than Co-exchanged product **3,** and **1** is completely inactive, *viz.*, the conversions of 89 and 76% for **2** and **3**, respectively. The results indicate that Cu(II)-containing complexes have good catalytic activities in the oxidative coupling reaction. The contrasting reaction using Cu $(NO_3)_2$ or $Co(NO_3)_2$ as catalyst only gives trace amounts of PPE. The reason is that the N/O donor ligands interact with metal ions to provide a delocalized electronic system within complexes, which induce the modification of the electronic properties of the molecules.

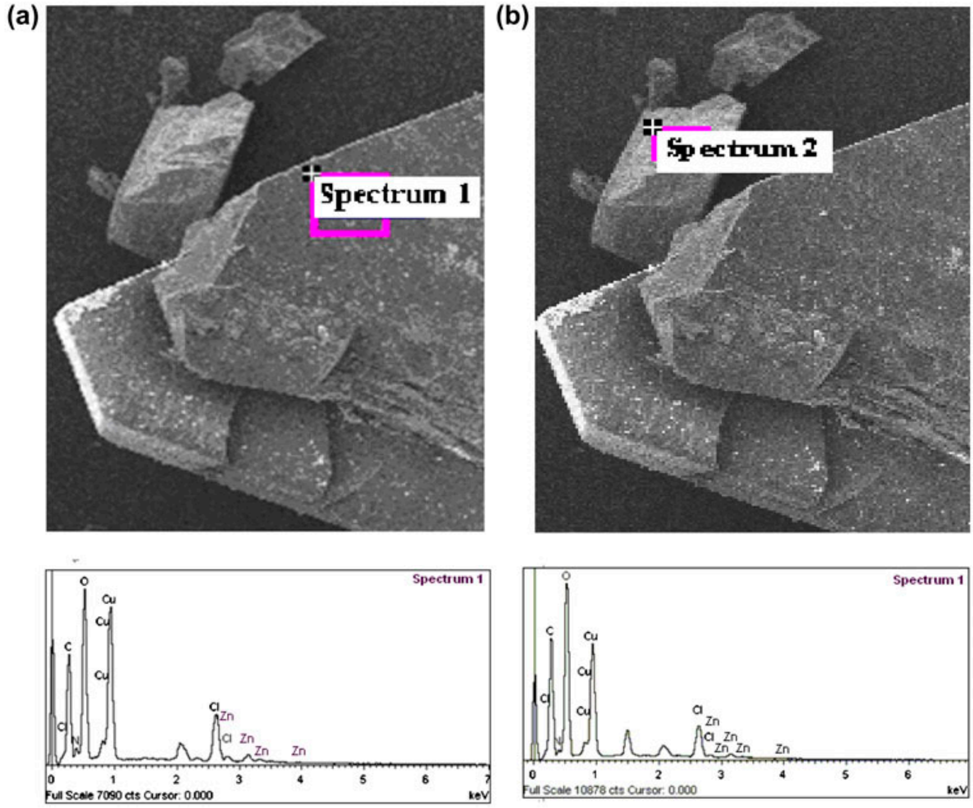

Figure 5. (a) SEM and EDS for the surface of **2**. (b) SEM and EDS for the interior of **2** after a single crystal is cut.

This favors the coordination of DMP to metal centers to form the proposed active metal species and the subsequent polymerization of DMP [24]. Likewise, Reedijk and co-workers have also shown that a series of Cu(II) complexes incorporating structurally related N,O containing ligands underwent this polymerization more efficiently than copper(II) salts [25]. This suggests that the copper complexes have an obvious comparative advantage in the oxidative coupling of DMP. In addition, central metal ion-exchanged products **2** and **3** perform identically with selectivity of almost 88%, which is comparable to that found for enzymes such as laccaese and tyrosinase [26].

The potential benefits of the heterogeneous catalyst include facilitation of catalyst separation from reagents and reaction products, and simplification of methods for catalyst recycling [27]. For a truly effective heterogeneous catalyst, therefore, it is critical that recovery can be simple and efficient, and that the recovered catalyst can retain its original reactivity through multiple cycles. As Cu-exchanged product **2** shows higher catalytic activity, we have tested for its recovery and reuse. After the reaction completed, the catalyst was recovered by filtration for consecutive runs. The recovered catalyst was used for a new reaction batch of DMP. Catalyst **2** exhibits excellent reusability for three times without showing any significant deterioration of catalytic activity. Then, we carried out another control reaction, because in the catalytic process, the leached metal species might catalyze efficiently the

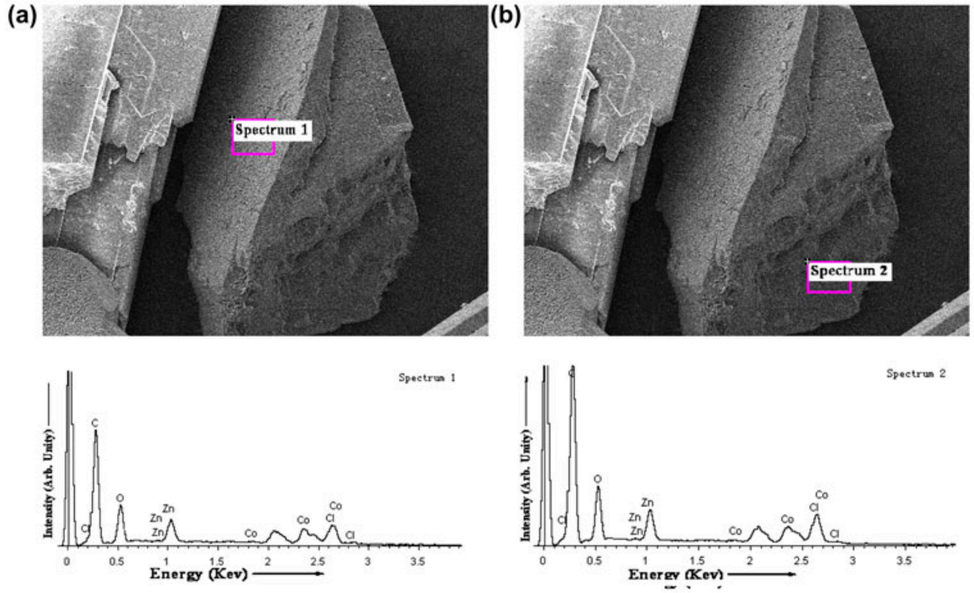

Figure 6. (a) SEM and EDS for the surface of **3**. (b) SEM and EDS for the interior of **3** after a single crystal is cut.

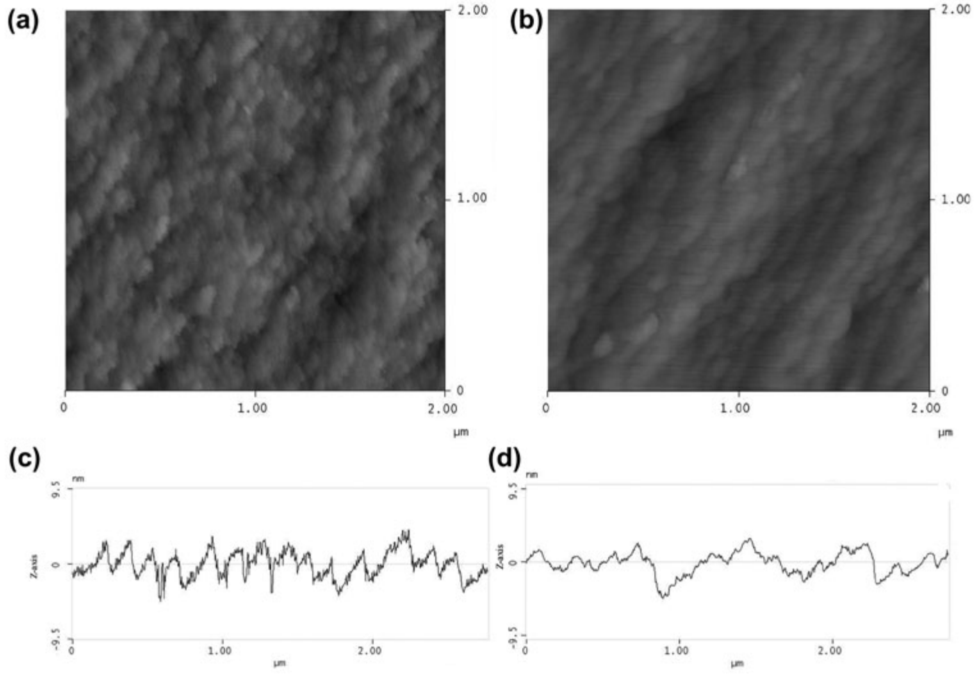

Figure 7. (a) Image of single crystal surface of **1**. (b) Image of single crystal surface of **2**. (c) Profile of single crystal surface of **1**. (d) Profile of single crystal surface of **2**.
Note: Different scale for *Z*-axis representing height of microcrystallites.

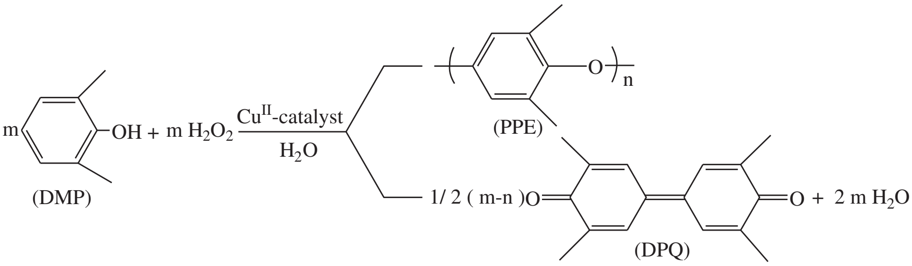

Scheme 1. Oxidative polymerization of DMP in water.

Table 2. Oxidative coupling of DMP in water[a] or in methanol–toluene mixture[b] catalyzed by **1–3**.

Catalysts	Solvent	Conversion (%)	Selectivity (%)
1	H_2O	0	0
	CH_3OH/toluene	0	0
2	H_2O	89	87.2
	CH_3OH/toluene	65	89.3
3	H_2O	76	86.4
	CH_3OH/toluene	52	87.8
[Cu(pc)(phen)(H_2O)]$_2$·5H_2O (**4**)	H_2O	96	90.4
	CH_3OH/toluene	87	91.8
[Co(pc)(phen)(H_2O)$_3$]·H_2O (**5**)	H_2O	86	89.6
	CH_3OH/toluene	70	91.2
Cu(NO_3)$_2$	H_2O	26	49
Co(NO_3)$_2$	H_2O	19	37

[a] Heterogeneous optimized conditions: DMP (1 mM), NaOH (1 mM), H_2O_2 (0.02 mL), and catalyst (0.02 mM) in 5 mL of water for 8 h at 50 °C.
[b] Homogeneous optimized conditions: DMP (1 mM), NaOMe (0.14 mM), H_2O_2 (0.05 mL), and catalyst (0.02 mM) in a 1.5 : 1 MeOH/toluene mixture (5 mL) for 3 h under the ambient temperature.

oxidative coupling reaction instead of the heterogeneous catalysts [28]. To examine this possibility, we filtered catalyst **2** after the oxidative polymerization and allowed the filtered catalyst and the filtrate to react with another aliquot of DMP, respectively, as shown in the previous study [28]. The filtered catalyst was subjected to the second run by charging with new reagents and then the products were again formed with about 85–92% of the original conversion. The filtrate obtained from the first filtration was also used in a new reaction with the addition of substrate. Only 6–9% conversion of DMP was observed under similar conditions. This result strongly suggests that the dominant reactive species is the heterogeneous catalyst **2**, not species such as the leached metal. However, about 6–9% conversion by the filtrate indicates that trace amounts of Cu metal ions might be leached during the catalysis. XRD pattern of the filtered catalyst after the reaction revealed the same pattern as the original catalyst, suggesting that the original structure of the filtered catalyst had been retained during the reaction. Based on these results, we have concluded that the heterogeneous catalyst **2** could be recycled multiple times without a significant loss of activity.

To fully understand the intrinsic advantage of heterogeneous *versus* homogeneous catalysts, the oxidation coupling of DMP is conducted in 1.5 : 1 (v/v) methanol–toluene mixed solution using central metal ion-exchanged products **2** and **3** as homogeneous catalysts under the same reaction conditions as the prior study (table 2) [17]. To our surprise, the use of central metal ion-exchanged products **2** and **3** acting as homogeneous catalysts can effectively suppress diphenoquinone production and improve the selectivity for PPE, while decreasing distinctly the catalytic activities. For example, when utilizing **2** as heterogeneous catalyst, the oxidation coupling of DMP occurs with 89% conversion and 87.2% selectivity for PPE. Nevertheless, **2** assumes the markedly lower efficiency (65% conversion) for the reaction in methanol–toluene medium, albeit with slightly enhanced selectivity of 89.3%. The superior activities of the complexes in the heterogeneous catalytic system may be attributed to full exposure of metal sites, therefore giving an ultimately high degree of metal dispersion [29]. Clearly, central metal ion exchange can be used to modify the catalysis properties of metal–organic complexes.

Furthermore, we evaluate catalytic efficiencies of pure copper complex **4** and cobalt complex **5** for comparison [30]. As can be seen in table 2, in spite of heterogeneous or homogeneous reaction systems, pure copper or cobalt complex **4** or **5** has superior catalytic activity to the cation-exchanged products **2** or **3**, and the activity and selectivity obtained with **4** are better than those observed using cobalt complex **5**. This observation is very significant since it prompts us to construct new self-assembly Cu-complexes as catalysts for the oxidative coupling of DMP. In addition, it is of note that all the catalysts used in this study, including the cation-exchanged products and pure complexes, show an identical product distribution for PPE and DPQ, signifying that all the catalysts probably carry out the oxidation coupling of DMP by the same reaction mechanism.

On the basis of the above experimental results and previous literature [31], a plausible reaction mechanism for the present oxidative coupling reaction was proposed as follows: DMP is dissolved in the basic aqueous phase to form the phenolate anion; these phenoxide anions coordinate to M(II) centers and then electron transfer from the coordinated phenoxide anions to M(II) ions occurs, leading to the formation of phenoxyl radicals. The resultant M(I) ions were re-oxidized to M(II) ions by H_2O_2 (M = Cu, or Co). The C–O coupling of these phenoxyl radicals yields the linear polymer PPE; the C–C coupling of these phenoxyl radicals results in the byproduct DPQ.

4. Conclusion

In crystalline state, **1** undergoes a partial metal ion exchange reaction and two SCTSC transformation products (**2** and **3**) are obtained. Using central metal ion-exchanged products **2** and **3** as catalysts, a green aqueous-medium catalytic oxidative coupling of DMP has been explored with potentials in “green chemistry and technology,” which suggests that central metal ion exchange might be a powerful and effective method to modify properties of crystalline materials only by varying central metal ions under moderate conditions.

Supplementary material

CCDC 961149–961151 contain the supplementary crystallographic data for **1** and its cation-exchanged products **2** and **3**, respectively. These data can be obtained free of charge from the Cambridge Crystallographic Data Center via www.ccdc.cam.ac.uk/data_request/cif.

Acknowledgements

This work was supported by a project funded by the Priority Academic Program Development of Jiangsu Higher Education Institutions (PAPD).

References

[1] A.S. Hay, H.S. Blanchard, G.F. Endres, J.W. Eustance. *J. Am. Chem. Soc.*, **81**, 6335 (1959).

[2] K. Saito, T. Masuyama, H. Nishide. *Green Chem.*, **5**, 535 (2003).

[3] J.M. DeSimone. *Science*, **297**, 799 (2002).

[4] C.J. Li, L. Chen. *Chem. Soc. Rev.*, **35**, 68 (2006).

[5] K. Saito, T. Tago, T. Masuyama, H. Nishide. *Angew. Chem. Int. Ed.*, **43**, 730 (2004).

[6] (a) H.K. Chae, D.Y. Siberio-Pérez, J.H. Kim, Y.B. Go, M. Eddaoudi, A.J. Matzger, M. O'Keeffe, O.M. Yaghi. *Nature*, **427**, 523 (2004); (b) M. Eddaoudi, D.B. Moler, H. Li, B. Chen, T.M. Reineke, M. O'Keeffe, O.M. Yaghi. *Acc. Chem. Res.*, **34**, 319 (2001); (c) R. Kitaura, K. Fujimoto, S. Noro, M. Kondo, S. Kitagawa. *Angew. Chem. Int. Ed.*, **41**, 133 (2002); (d) E. Burkholder, V. Golub, C.J. ÓConnor, J. Zubieta. *Chem. Commun.*, **2003**, 2128 (2003); (e) S.S. Kaye, J.R. Long. *J. Am. Chem. Soc.*, **127**, 6506 (2005).

[7] (a) K.S. Min, M.P. Suh. *J. Am. Chem. Soc.*, **122**, 6834 (2000); (b) M. Dinca, J.R. Long. *J. Am. Chem. Soc.*, **129**, 11172 (2007).

[8] L. Pan, H. Liu, X. Lei, X. Huang, D.H. Olson, N.J. Turro, J. Li. *Angew. Chem. Int. Ed.*, **42**, 542 (2003).

[9] (a) M. Albrecht, M. Lutz, A.L. Spek, G. van Koten. *Nature*, **406**, 970 (2000); (b) S.E. Castillo-Blum, N. Barba-Behrens. *Coord. Chem. Rev.*, **196**, 3 (2000); (c) E. Burkholder, V. Golub, C.J. ÓConnor, J. Zubieta. *Inorg. Chem.*, **43**, 7014 (2004).

[10] Z.Z. Lin, F.L. Jiang, D.Q. Yuan, L. Chen, Y.F. Zhou, M.C. Hong. *Eur. J. Inorg. Chem.*, **2005**, 1927 (2005).

[11] (a) D.H. Son, S.M. Hughes, Y.D. Yin, A.P. Alivisatos. *Science*, **306**, 1009 (2004); (b) R.D. Robinson, B. Sadtler, D.O. Demchenko, C.K. Erdonmez, L.W. Wang, A.P. Alivisatos. *Science*, **317**, 355 (2007); (c) M.J. Manos, R.G. Iyer, E. Quarez, J.H. Liao, M.G. Kanatzidis. *Angew. Chem. Int. Ed.*, **44**, 3552 (2005); (d) N. Ding, D.Y. Chung, M.G. Kanatzidis. *Angew. Chem. Int. Ed.*, **45**, 1397 (2006); (e) M.J. Manos, C.D. Malliakas, M.G. Kanatzidis. *Chem.-Eur. J.*, **13**, 51 (2007); (f) M.J. Manos, K. Chrissafis, M.G. Kanatzidis. *J. Am. Chem. Soc.*, **128**, 8875 (2006).

[12] (a) J.L. Atwood, L.J. Barbour, A. Jerga, B.L. Schottel. *Science*, **298**, 1000 (2002); (b) K. Biradha, M. Fujita. *Angew. Chem. Int. Ed.*, **41**, 3392 (2002); (c) K. Biradha, Y. Hongo, M. Fujita. *Angew. Chem. Int. Ed.*, **41**, 3395 (2002); (d) B. Rather, M.J. Zaworotko. *Chem. Commun.*, **2003**, 830 (2003); (e) D. Maspochi, D. Ruiz-Molina, K. Wurst, N. Domingo, M. Cavallini, F. Biscarini, J. Tejada, C. Rovira, J. Veciana. *Nat. Mater.*, **2**, 190 (2003); (f) H.J. Choi, M.P. Suh. *J. Am. Chem. Soc.*, **126**, 15844 (2004).

[13] (a) L.W. Mi, H.W. Hou, Z.Y. Song, H.Y. Han, Y.T. Fan. *Chem.-Eur. J.*, **14**, 1814 (2008); (b) L.W. Mi, H.W. Hou, Z.Y. Song, H.Y. Han, H. Xu, Y.T. Fan, S.W. Ng. *Cryst. Growth Des.*, **7**, 2553 (2007); (c) J. Wu, H.W. Hou, H.Y. Han, Y.T. Fan. *Inorg. Chem.*, **46**, 7960 (2007); (d) J.A. Zhao, L.W. Mi, J.Y. Hu, H.W. Hou, Y.T. Fan. *J. Am. Chem. Soc.*, **130**, 15222 (2008); (e) S. Das, H. Kim, K. Kim. *J. Am. Chem. Soc.*, **131**, 3814 (2009); (f) Z.Q. Wang, S.M. Cohen. *Chem. Soc. Rev.*, **38**, 1315 (2009).

[14] A.X.S. Bruker. *SAINT Software Reference Manual*, Bruker AXS Inc., Madison, WI (1998).

[15] G.M. Sheldrick. *SADABS, Siemens Area Detector Absorption Corrected Software*, University of Göttingen, Germany (1996).

[16] G.M. Sheldrick. *SHELXTL NT, Version 5.1; Program for Solution and Refinement of Crystal Structures*, University of Göttingen, Germany (1997).

[17] B. Xiao, H.W. Hou, Y.T. Fan. *J. Organomet. Chem.*, **692**, 2014 (2007).

[18] (a) K.L. Zhang, Y. Chang, S.W. Ng. *Inorg. Chim. Acta*, **368**, 49 (2011); (b) G.A. Farnum, J.S. Lucas, C.Y. Wang, R.L. LaDuca. *Inorg. Chim. Acta*, **368**, 84 (2011).

[19] (a) L.K. Li, Y.L. Song, H.W. Hou, Y.T. Fan, Y. Zhu. *Eur. J. Inorg. Chem.*, **2005**, 3238 (2005); (b) G. Li, H.W. Hou, L.K. Li, X.R. Meng, Y.T. Fan, Y. Zhu. *Inorg. Chem.*, **42**, 4995 (2003); (c) H.W. Hou, L.K. Li, G. Li, Y.T. Fan, Y. Zhu. *Inorg. Chem.*, **42**, 3501 (2003); (d) J.P. Li, Y.L. Song, H.W. Hou, M.S. Tang, Y.T. Fan, Y. Zhu. *J. Organomet. Chem.*, **692**, 1584 (2007).

[20] (a) N. Rodriguez-Hornedo, D. Murphy. *J. Pharm. Sci.*, **88**, 651 (1999); (b) J. Booth, R.G. Compton, J.H. Atherton. *J. Phys. Chem. B*, **102**, 3980 (1998); (c) J. Booth, Q. Hong, R.G. Compton, K. Prout, R.M. Payne. *J. Colloid Interface Sci.*, **192**, 207 (1997); (d) A.N. Khlobystov, N.R. Champness, C.J. Roberts, S.J.B. Tendler, C. Thompson, M. Schröder. *CrystEngComm.*, **4**, 426 (2002); (e) C. Thompson, N.R. Champness, A.N. Khlobystov, C.J. Roberts, M. Schröder, S.J.B. Tendler, M.J. Wilkinson. *J. Microsc.*, **214**, 261 (2004).

[21] (a) C.M. Pina, L. Fernández-Díaz, M. Prieto, A. Putnis. *Geochim. Cosmochim. Acta*, **64**, 215 (2000); (b) A.J. Malkin, Y.G. Kuznetsov, A.J. McPherson. *J. Cryst. Growth*, **196**, 471 (1999).

[22] (a) F. Robinson, M.J. Zaworotko. *J. Chem. Soc., Chem. Commun.*, **1995**, 2413 (1995); (b) O.M. Yaghi, H. Li, C. Davis, D. Richardson, T.L. Groy. *Acc. Chem. Res.*, **31**, 474 (1998); (c) K.S. Min, M.P. Suh. *J. Am. Chem. Soc.*, **122**, 6834 (2000).
[23] (a) H.Y. Han, S.J. Zhang, H.W. Hou, Y.T. Fan, Y. Zhu. *Eur. J. Inorg. Chem.*, **2006**, 1594 (2006); (b) M.R. Maurya, I. Jain, S.J. Titinchi. *Appl. Catal. A: Gen.*, **249**, 139 (2003).
[24] (a) P. Gamez, C. Simons, R. Steensma, W.L. Driessen, G. Challa, J. Reedijk. *Eur. Polym. J.*, **37**, 1293 (2001); (b) S. Tanase, P.M. Gallego, E. Bouwman, G.J. Long, L. Rebbouh, F. Grandjean, R. Gelder, I. Mutikainen, U. Turpeinen, J. Reedijk. *Dalton Trans.*, 1675 (2006).
[25] S.J.A. Guieu, A.M.M. Lanfredi, C. Massera, L.D. Pachón, P. Gamez, J. Reedijk. *Catal. Today*, **96**, 259 (2004).
[26] G. Pandey, C. Muralikrishna, U.T. Bhalerao. *Tetrahedron Lett.*, **31**, 3771 (1990).
[27] Y. Kim, S.K. Choi, S.M. Park, W. Nam, S.J. Kim. *Inorg. Chem. Commun.*, **5**, 612 (2002) and references therein .
[28] (a) S.K. Yoo, J.Y. Ryu, J.Y. Lee, C. Kim, S.J. Kim, Y. Kim. *Dalton Trans.*, 1454 (2003); (b) S.J. Hong, J.Y. Ryu, J.Y. Lee, C. Kim, S.J. Kim, Y. Kim. *Dalton Trans.*, 2697 (2004).
[29] U. Mueller, M. Schubert, F. Teich, H. Puetter, K. Schierle-Arndt, J. Pastré. *J. Mater. Chem.*, **16**, 626 (2006).
[30] (a) B. Xiao. *Z. Kristallogr. NCS*, **227**, 149 (2012); (b) B. Xiao. *Z. Kristallogr. NCS*, **227**, 125 (2012).
[31] (a) C. Boldron, G. Aromí, G. Challa, P. Gamez, J. Reedijk. *Chem. Commun.*, **2005**, 5808 (2005); (b) K. Saito, T. Tago, T. Masuyama, H. Nishide. *Angew. Chem. Int. Ed.*, **43**, 730 (2004); (c) P.J. Baesjou, W.L. Driessen, G. Challa, J. Reedijk. *J. Am. Chem. Soc.*, **119**, 12590 (1997); (d) J. Gao, J.H. Reibenspies, A.E. Martell. *Inorg. Chim. Acta*, **338**, 157 (2002).